Received: 3 November 2023 | Revised: 22 April 2024 | Accepted: 14 May 2024

DOI: 10.1111/ejss.13516

RESEARCH ARTICLE

European Journal of Soil Science WILEY

Greenhouse gas fluxes of microbial-induced calcite precipitation at varying urea-to-calcium concentrations

Carla Comadran-Casas[1,2] | **Nicolas Brüggemann**[3] | **M. Ehsan Jorat**[2]

[1]James Watt School of Engineering, University of Glasgow, Glasgow, UK

[2]School of Applied Science, Abertay University, Dundee, UK

[3]Institute of Bio- and Geosciences—Agrosphere (IBG-3), Forschungszentrum Jülich GmbH, Jülich, Germany

Correspondence
Carla Comadran-Casas, Advanced Research Centre, University of Glasgow, 11 Chapel Ln, Glasgow, G11 6EW, Scotland, UK.
Email: carla.comadrancasas@glasgow.ac.uk

Funding information
Scottish Alliance for Geoscience, Environment and Society; Research-led Innovation Nodes for Contemporary Society; Norman Fraser Design Trust

Abstract

Microbial-induced calcite precipitation (MICP) is regarded as environmentally friendly, partly due to the storage of carbon as carbonates. Although CO_2 emissions during MICP have been reported, quantification of its environmental impact regarding total greenhouse gas fluxes has not yet been thoroughly investigated. In particular, N_2O fluxes could occur in addition to CO_2 since MICP involves the microbially mediated nitrogen cycle. This study investigated the greenhouse gas fluxes during biostimulation of MICP in quartz sand in incubation experiments. Soil samples were treated with MICP cementation solution containing calcium concentrations of 0, 20, 100 and 200 mM at a fixed urea concentration of 100 mM to offer a range of carbonation potential and/or mitigation of CO_2 emissions. Greenhouse gas (CO_2, CH_4 and N_2O) measurements were determined by gas chromatography during incubations. Soil total inorganic carbon and the isotopic composition of precipitated and emitted CO_2 were determined by isotope ratio mass spectrometry. CO_2 emissions (0.52 to 4.08 μg of CO_2–C h^{-1} g^{-1} soil) resulted from MICP, while N_2O and CH_4 fluxes were not detected. Increasing Ca^{2+} with respect to urea resulted in lower CO_2 emissions, lower solution pH, similar carbonate precipitation and urea hydrolysis inhibition. The highest urea-to-calcium ratio (1:0.2) emitted roughly two times the amount of CO_2 (112 μg of CO_2–C g^{-1} soil) compared to the 1:1 and 1:2 ratios (47 to 58 μg of CO_2–C g^{-1} soil) and five to six times more than samples that did not receive Ca^{2+} (1:0) (∼18 μg of CO_2–C g^{-1} soil). Precipitated $CaCO_3$–C was tenfold higher than cumulative emitted CO_2–C, and isotopic analysis indicated both emitted and precipitated carbon were of urea origin. Both emitted and precipitated carbon accounted for a very low percentage of total carbon applied in the system (<0.35 and <4.5%, respectively), presumably due to limited urea hydrolysis which was negatively affected by increasing the Ca^{2+} concentration.

KEYWORDS

carbon dioxide, carbon stable isotopes, carbonate, CO_2 emissions, greenhouse gas fluxes, MICP

1 | INTRODUCTION

In the current context of human-induced global warming (IPCC, 2021), environmental pollution, and biodiversity decline (IPBES, 2019), the environmental impact of current and future anthropogenic activities requires careful consideration. Over the past 25 years, microbial-induced calcite precipitation (MICP) via urea hydrolysis has been developing as an alternative to traditional approaches in soil and environmental engineering, mainly in soil stabilisation, manufacturing (e.g., bricks) and repair (concrete fissures) of construction materials, and bioremediation of contaminants in soil (Al Qabany et al., 2012; Castro-Alonso et al., 2019; DeJong et al., 2006; Fang et al., 2021; Fujita et al., 2004; Montoya et al., 2014; Stocks-Fischer et al., 1999; Warren et al., 2001; Whiffin et al., 2007; Zamani & Montoya, 2018).

The construction sector is one of the largest energy consuming (36%) and carbon dioxide (CO_2) emitting (39%) sectors globally (IEA, 2020). Manufacturing of materials (e.g., cement) accounts for 11% of total CO_2 emissions of the construction sector (IEA, 2020). In particular for soil engineering, cement and chemical binders are widely used for soil stabilisation (Chang et al., 2019), with ground improvement processes (mixing and grouting) contributing to 0.2% of global CO_2 emissions (Chang et al., 2016). Strategies to minimise CO_2 emissions associated with soil engineering practices are therefore necessary. MICP is also relevant in the context of soil science since the biogeochemical process of urea hydrolysis is the same as that occurring in agricultural settings with the application of nitrogen (N) fertilisers such as urea. The agricultural sector is estimated to be responsible for up to 8.5% of global greenhouse gas (GHG) emissions (IPCC, 2019). Synthetic nitrogen fertiliser is estimated to account for 1129.1 ± 171.1 Mt CO_{2e} emissions, ~38% from industrial manufacturing and 58% from direct (CO_2) and indirect (N_2O) emissions associated to urea application to agricultural soils worldwide (Menegat et al., 2022).

In the literature, MICP is widely regarded as a 'sustainable' and 'environmentally friendly' technique compared to traditional approaches relying on carbon intensive materials (e.g., involving cement), although there is a lack of data on the environmental impact and sustainability of the technique. Several aspects favour this perception: MICP is a low energy technique since low viscosity of treatment fluid (water) greatly reduces the requirement for high injection pressures; the chemicals used are not associated with carbon intensive industries such as the cement industry, with global contribution to CO_2 emissions of 5 to 7% (Benhelal et al., 2013); and the technique relies on naturally occurring biogeochemical processes. Nonetheless, production of calcium chloride and urea, the main components of MICP via urea hydrolysis, is associated with energy intensive processes fuelled by combustion of fossil fuels. Calcium chloride is produced by combustion of calcium carbonate rocks (e.g., limestone) which requires temperatures above 700°C, releasing 440 g of CO_2 per kg of $CaCO_3$ breakdown excluding emissions derived from energy input. Urea is produced in two steps where, first, natural gas largely containing methane is partially oxidised with O_2 to produce CO_2 (900–1200°C, 40–100 bar), and H_2 is combined with N_2 to produce NH_3 through the Haber–Bosch process. The second step combines NH_3 and CO_2 to produce urea (Pagani & Zardi, 1995). A recent life cycle assessment (LCA) of MICP assumed that all carbon introduced in the system is precipitated as calcium carbonate (Deng et al., 2021). However, it is likely that MICP in field case scenarios does not achieve complete conversion of urea–C into precipitated calcium carbonate. This constitutes a gap in the literature as data on soil-atmosphere GHG fluxes of MICP is scarce.

MICP via urea hydrolysis is a heterotrophic microbial pathway which produces CO_2 and NH_3 gases as by-products of microbial activity. Okyay et al. (2016) and Okyay and Rodrigues (2015) investigated biotic and abiotic CO_2 fluxes during MICP in aqueous samples obtained from travertine cave environments in incubation experiments at a concentration of 10% CO_2 in the vial headspace. They posed the relevant question of whether the amount of CO_2 produced by bacterial metabolism would exceed the bacterial capability to sequester CO_2 through MICP. Results of biotic experiments highlighted CO_2 sequestration (0.9% to up to 8.6% of CO_2 in vial headspace), but also CO_2 emissions, the net balance being directly dependant on microbial composition. Abiotic experiments elucidated concomitant CO_2 sequestration due to the alkalinity of solution pH, composition and nutrient concentration in treatment media. In a former study, we investigated soil-atmosphere CO_2 gas fluxes over 2 months during and following biostimulation of MICP on a quartz sand using calcium chloride or dolerite fines (basaltic rock composed of calcium-rich minerals by-product of the quarrying sector) as sources of calcium for MICP. Our

Highlights

- The study determines MICP related soil-atmosphere greenhouse gas fluxes.
- During MICP net CO_2 emissions occur, but no N_2O nor CH_4 fluxes were observed.
- Increasing Ca^{2+}-to-urea ratio resulted in lower CO_2 emissions and similar carbonate precipitation.
- Urea-to-Ca^{2+} ratio of 1:1 lowered CO_2 emissions and maintained soil carbonation.

results highlighted net CO_2 emissions during and following MICP treatment, which were dependant on reaction time and soil water saturation conditions (i.e., submerged vs freely drained) (Casas et al., 2020). Our experiment was conducted at a fixed urea-to-calcium molar ratio (100 and 20 mM, respectively). Because the molar content of calcium was smaller than urea–C, calcium could have limited the extent of soil carbonation and the capacity of the system to balance CO_2 emissions.

An unexplored aspect of MICP is that release of NH_3 from urea degradation into the soil solution presents the potential occurrence of nitrite, nitrate, and nitrous oxide (N_2O) emissions through microbial nitrification and denitrification processes. Excess of nitrate is widely recognised as environmentally detrimental to underground water quality and life due to eutrophication, while the estimated global warming potential of N_2O is 265 times that of CO_2 over a 100-year period (IPCC, 2019). Studies on potential nitrification following MICP have received little attention, despite Gat et al. (2016) observing ammonia oxidation (production of nitrate) nearly a month following MICP treatment, demonstrating the potential for occurrence of N_2O emissions.

To expand the work conducted by Okyay et al. (2016), Okyay and Rodrigues (2015) and Casas et al. (2020), in this study we present an investigation on the GHG (CO_2, N_2O and CH_4) fluxes during biostimulation of MICP in a quartz sand in incubation experiments. The aims were, on the one hand, to determine whether N_2O gas emissions could result from MICP and, on the other hand, to study the dynamics of CO_2 fluxes during MICP under different conditions to determine whether CO_2 emissions could be reduced, balanced, or whether MICP in soil could act as a net sink of CO_2. To do so, we varied the urea-to-calcium molar ratio by varying calcium and fixing urea concentration in treatment solution to provide a range of soil carbonation and CO_2 sequestration potential, under the hypotheses that with increasing calcium concentration more $CaCO_3$ would precipitate, and less CO_2 would be emitted. In addition, we studied the abiotic effect of alkaline pH, induced by urea hydrolysis, on CO_2 sequestration versus microbial-derived CO_2 emissions. Furthermore, the isotopic composition of precipitated and emitted CO_2 were investigated to elucidate the origin of precipitated and emitted CO_2.

2 | MATERIALS AND METHODS

2.1 | Soil sampling and characterisation

Sand was obtained from a quarry located in the Lower Rhine Basin, Germany (50°55′018.8184″, 06°46′45.6528″, WGS84; operated by Quarzwerke GmbH, Frechen). The sampling location was selected close to vegetation (Figure S1) to ensure the soil was biologically active. The first 3 cm of the surface soil were removed, and the underlying soil was collected to a depth of 20 cm and sealed to prevent moisture loss. The sample consisted of a loose, homogeneous, white-greyish fine sand, with no presence of gravels, boulders, or fines. The soil water content was determined gravimetrically upon arrival at the laboratory. The grain size distribution was determined by wet sieving on two analytical replicates (ISO 11277: 1998), and the soil pH was determined in 0.01 M $CaCl_2$ in distilled water solution at a soil-to-solution ratio of 2.5:1 (Houba et al., 2000) on three analytical replicates (WTW SenTix 41 PLUS probe with WTW multi 340i pH meter, WTW, Weilheim, Germany; calibrated to pH = 4 and 7).

2.2 | MICP treatment solutions

MICP was induced through biostimulation of soil indigenous bacteria. The growth solution contained 1 g L^{-1} of cane molasses (MLS) (Rapunzel Naturkost GmbH, Germany), 0.1 g L^{-1} yeast extract (Vitasan Bio-Hefeextrakt; VITAM Hefe-Produkt GmbH, Germany), 100 mM anhydrous sodium acetate (CH_3COONa) (ACS, Merck KGaA, Germany) and 250 mM urea (≥99.5%, Carl Roth GmbH C Co., KG, Germany) in distilled water. The cementation solution contained 0.1 g L^{-1} of MLS, 100 mM sodium acetate, 100 mM urea and 0, 20, 100 or 200 mM calcium chloride dihydrate ($CaCl_2 \cdot 2H_2O$) (ACS, Merck KGaA, Germany) in distilled water. Ammonium was excluded from treatment solution as it has been reported not to be necessary for growth of ureolytic bacteria *Sporosarcina pasteurii* (Lapierre et al., 2020), and was shown not to prevent urea hydrolysis by indigenous bacteria by a previous study on this soil (Casas et al., 2020).

2.3 | MICP experiments

Greenhouse gas fluxes during MICP at varying urea-to-calcium ratios were investigated in an incubation experiment by gas chromatography. Treatments included distilled water (0:0) (control), MICP treatment solutions with varying concentrations of urea-C to calcium (Ca^{2+}) molar ratios (1:0, 1:0.2, 1:1 and 1:2), and a sodium hydroxide (NaOH) solution of adjusted pH of 9.5 used to study the abiotic GHG fluxes at the pH levels induced by the urea hydrolysis reaction (NaOH). Three replicate soil samples were prepared for each treatment by adding a constant mass of 1.5 g wet soil (m_{dry} = 1.1637 ± 0.0004 g;

$\theta = 22.4\%$; $n = 18$) in 22-mL gas chromatography vials. Solution was applied at a soil-solution ratio of 1:1.

The treatment sequence comprised a growth and a cementation phase. Initially, treatments that included urea (i.e., urea-to-calcium molar ratios 1:0, 1:0.2, 1:1, 1:2) received the growth solution, while control (0:0) and the abiotic (NaOH) treatments received distilled water. Aliquots were decanted after a reaction time (t_r) of 96 h. The cementation phase started 2 h after decantation and comprised five cementation solution (i.e., 0:0, 1:0, 1:0.2, 1:1, 1:2 and NaOH) applications. The first four applications were performed every 24 h on consecutive days. After each application, vials were sealed with butyl rubber septa and aluminium caps and incubated for a reaction time (t_r) of 10 h. After each incubation, vials were opened, aliquots decanted, and vials were stored at room temperature covered with aluminium foil until the next cementation solution was applied. The fifth cementation solution was applied 2 h after finalising the fourth incubation and was allowed to react for 24 h, where the incubation for the GC measurement lasted 10 h from $t_r = 14$–24 h. At the end of the incubation experiment, vials containing soil samples were oven-dried to a constant mass at 105°C for more than 24 h. Soil samples were subsequently obtained for quantification of soil total inorganic carbon and stable isotopes of soil carbonates (see Section 2.5).

The experiment was replicated in 22-mL vials using 5 g of soil (m_{wet}) to determine the pH of the soil aqueous phase simultaneously with gas measurements (see Section 2.4). An additional replicate experiment was run in 12-mL vials with screw-top exetainers sealed with septa using 0.1 g soil (m_{wet}) to determine the isotope composition of evolved CO_2–C in the vial headspace. A single gas measurement was carried out at the end of each 10 h incubation. The isotope analysis of evolved CO_2 was conducted as specified in Section 2.5.

2.4 | Gas measurements

A gas chromatograph (GC Clarus 590, PerkinElmer, Rodgau, Germany) equipped with an Elite Plot-Q column (20 m × 0.53 mm id × 20 μm), a flame ionisation detector (FID) and an electronic capture detector (ECD), interfaced to an autosampler (Turbo Matrix 110, PerkinElmer) was used to determine CO_2, CH_4 and N_2O concentration in the vial headspace during incubations using nitrogen as a carrier gas.

Gas measurements of the first four cementation applications were taken at $t_r = 1$, 4, 7 and 10 h and during the fifth application at $t_r = 15$, 19, 21 and 24 h. During the 10-h incubation time, four gas measurements were made on the same vial. The sampling procedure of the GC involved injecting N_2 into the vial until an overpressure of 1 bar was achieved prior to sampling 10% of the headspace volume. Therefore, the pressure drop within the vial was constant, whereas the amount of air remaining in the vial after each measurement was 90% of the air prior to the measurement. Gas concentration measurements were corrected by calculating the gas concentration equivalent to the initial amount of air as follows:

$$[C]_{corr,i} = [C]_{meas,\ i} / f_{air}^{\ m-1} \quad (1)$$

where $[C]_{corr}$ is the corrected gas concentration of the i gas (ppm or ppb), $[C]_{meas}$ is the measured gas concentration of the i gas (ppm or ppb), f_{air} is the fraction of air remaining after each measurement, equal to 0.9, and m is an integer that represents the gas measurement number and takes values of 1 for the first measurement, 2 for the second, and so on (for further details see Table S3). Corrected gas concentrations were used to calculate variations in gas concentrations in the vial headspace and, subsequently, gas fluxes. To compute gas fluxes, variations in gas concentration data were fitted to linear and convex quadratic equations. The polynomial fit was selected over the linear if the following three conditions were met: the coefficient of determination of polynomial fit (R^2_{pol}) was >0.8, the quadratic fit was convex ($a > 0$), indicating saturation of the gas in the vial headspace, and $R^2_{pol} > R^2_{lin}$. Cumulative emissions were calculated by multiplying the gas fluxes obtained from the linear or polynomial regressions by the incubation time ($t = 10$ h).

2.5 | Quantitative and isotopic analysis of carbon

Total organic carbon (TOC), total nitrogen (TN) and the isotopic signature of organic carbon ($\delta^{13}C_{TOC}$) in soil and carbon-containing compounds used for the preparation of growth and cementation solutions (i.e., molasses, urea, and sodium acetate) were determined in triplicate by elemental analysis–isotope ratio mass spectrometry (EA-IRMS) using an elemental analyser (EA; Flash 2000, Thermo Fisher Scientific, Bremen, Germany), interfaced with a continuous flow IRMS (CF-IRMS; Delta V Advantage, Thermo Fisher Scientific). Soil total inorganic carbon (TIC) and the C and O isotopic composition of precipitated carbonate ($\delta^{13}C_{TIC}$ and $\delta^{18}O$, respectively), and evolved CO_2 ($\delta^{13}C_{CO2}$) in vial headspace during incubations were determined by gas

chromatography–continuous flow–isotope ratio mass spectrometry (GC-CF-IRMS, GasBench II interfaced with a Delta V Advantage, Thermo Fisher Scientific). Soil TOC and TIC were determined in separate runs. For analysis of soil TOC, TIC was previously removed by fumigation of pre-weighed samples with concentrated hydrochloric acid vapour (Ramnarine et al., 2011). Soil TIC was determined by analysis of evolved CO_2 gas released by the reaction of carbonate and pure phosphoric acid (Debajyoti & Skrzypek, 2007). Evolved CO_2 in the vial headspace was estimated by comparing peak areas of samples against air samples. Certified isotopic standards were used for ^{13}C, referenced against the Vienna Pee Dee Belemnite (VPDB) scale.

3 | RESULTS

3.1 | Material characterisation

The soil used in this study was the same as used in Casas et al. (2020). The soil classified as poorly graded sand (SP, Unified Soil Classification System) with 29% medium, 67% fine sand, and fines content <4% (Figure S2). Soil organic C ($C_{TOC} = 0.0211$ wt%) and carbonate ($C_{TIC} = 0.0003$ wt%) content were very low, the C:N ratio was 13 and the soil pH was slightly acidic (pH = 6.4). The isotopic signature of soil inorganic and organic C was $\delta^{13}C_{TIC} = -13.9‰$ and $\delta^{13}C_{TOC} = -25.7‰$, respectively (Table S1). C-containing compounds used for the preparation of the growth and cementation solutions had a similar organic carbon content ($C_{org} = 20–32\%$), while the C_{org} isotopic signature differed ($\delta^{13}C_{urea} = -40‰$, $\delta^{13}C_{Na\text{-}Ac} = -31‰$ and $\delta^{13}C_{MLS} = -13‰$) (Table S2).

3.2 | Solution pH

Soil solution pH data are presented in Figure 1. At the end of the growth phase ($t = 0$), pH ranged from 8.9 to 9.2 for all treatments containing urea, indicating similar production of ammonium ions through urea hydrolysis by soil indigenous ureolytic microbial communities. The pH of control samples (0:0) was generally between 6.2 and 6.7, similar to the untreated quartz sand (pH = 6.4, Table S1). Abiotic samples (NaOH) showed stable pH values of about 9 throughout, a decrease of 0.5 units compared to the NaOH solution (pH = 9.5). The pH of MICP treatments (1:0, 1:0.2, 1:1 and 1:2) was alkaline, ranging from 7 to 9. Lower pH was measured with increasing Ca^{2+} concentration: samples that did not receive Ca^{2+} (1:0) showed a stable value at a pH of about 9 during incubations, similar to NaOH samples. Instead, samples that received Ca^{2+} (1:0.2, 1:1 and 1:2), showed a decreasing pH trend, stabilising at lower pH with increasing Ca^{2+} (i.e., approx. 8, 7.5 and 7.3 for urea-to-calcium molar ratios 1:0.2, 1:1 and 1:2, respectively). pH dropped during reaction time $t_r = 1$ to 4 h and flattened from $t_r = 4$ to 10 h. pH drops were less pronounced as the number of cementation solutions applied increased. For example, during the fourth incubation period ($t = 72–82$ h), the pH showed flatter trends than during the first incubation period ($t = 0–10$ h). Flattening of pH trends was observed earlier with increasing the Ca^{2+} content: for 1:0.2 samples,

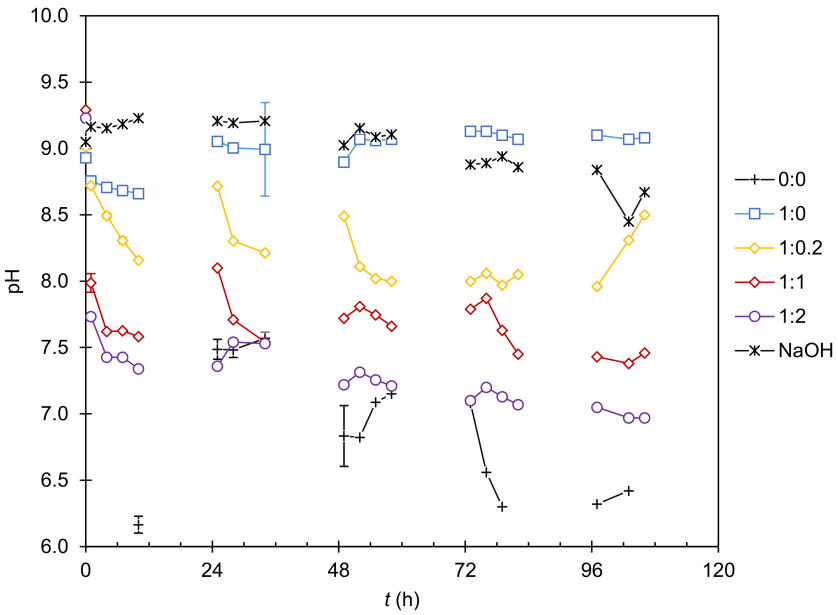

FIGURE 1 Soil solution pH during biostimulation of MICP in quartz sand treated with distilled water (0:0, control), urea-to-calcium molar ratios 1:0, 1:0.2, 1:1, 1:2, and solution of adjusted pH of 9.5 with sodium hydroxide (NaOH). pH measurements conducted over 10 h incubation periods at reaction time (t_r) of 1, 4, 7 and 10 h during the first four incubations ($t = 0–82$ h), and at $t_r = 15$, 19, 21 and 24 h during the fifth incubation ($t = 84–108$ h), coinciding with greenhouse gases measurements in parallel experiment. Markers and error bars indicate the average and standard deviation of three replicate samples.

flattening was observed during the fourth incubation period (t = 72–82 h), while for 1:2 samples flattening occurred during the second incubation period (t = 24–34 h). An increasing trend in pH was recorded for urea-to-calcium molar ratio of 1:0.2 during the fifth incubation period (t_r = 14 to 24 h), where pH increased over time, while treatments with higher Ca^{2+} content (1:1 and 1:2) showed a stable pH.

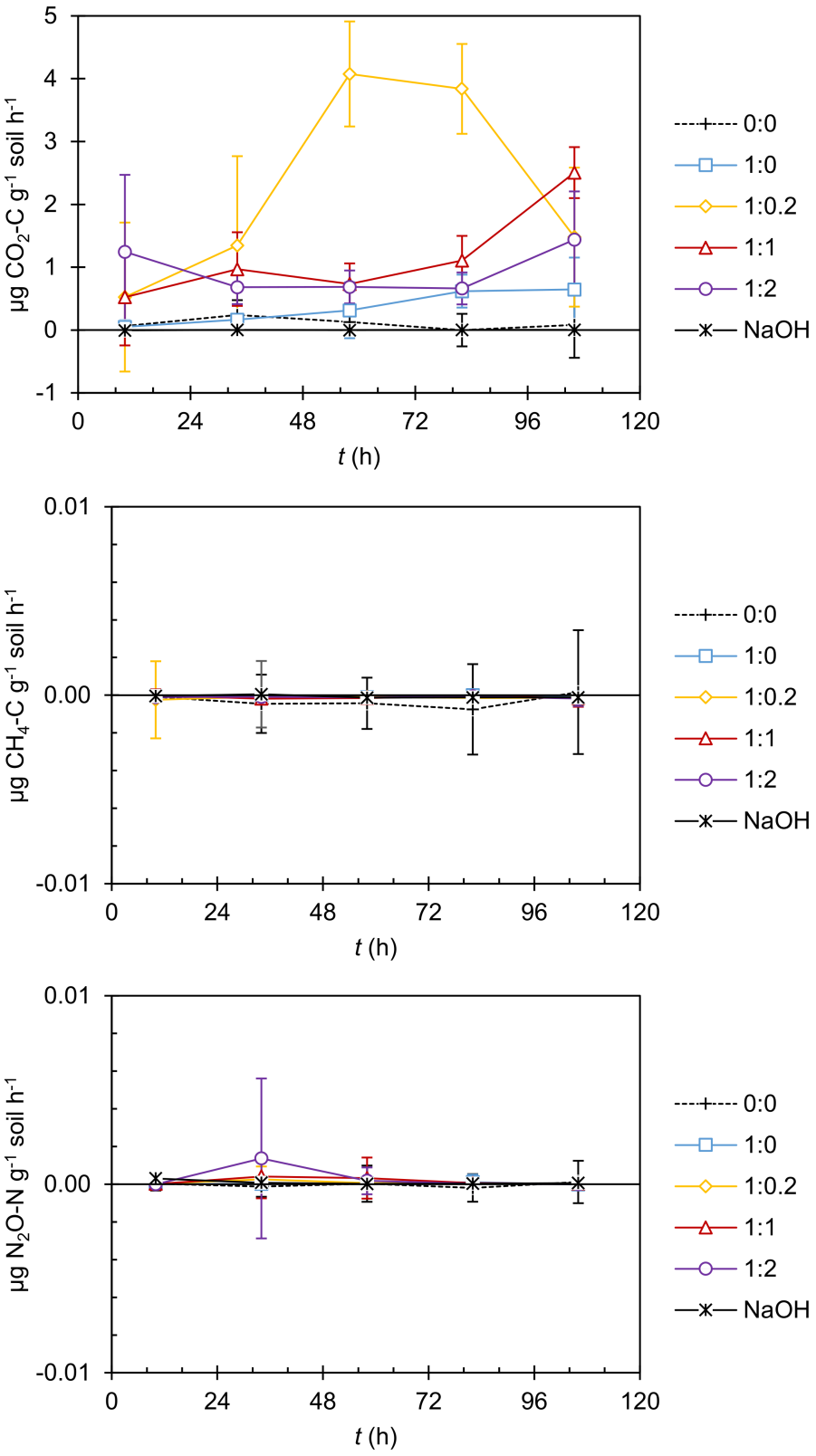

FIGURE 2 Greenhouse gas (a: CO_2–C; b: N_2O–N; c: CH_4–C) fluxes during biostimulation of MICP in fine quartz sand after application of solutions with different urea-to-calcium molar ratios (1:0, 1:0.2, 1:1 and 1:2), distilled water (0:0), and distilled water with pH of 9.5 adjusted with sodium hydroxide (NaOH) calculated from headspace concentrations of CO_2, N_2O and CH_4, measured by gas chromatography, during incubations in gas-tight vials at t = 1, 4, 7 and 10 h. Markers and error bars indicate the average and standard deviation of three replicate samples.

3.3 | Greenhouse gas fluxes

Figure 2 presents calculated GHG fluxes of CO_2–C, CH_4–C, and N_2O–N during MICP at varying urea-to-calcium molar ratios, where positive values indicate emissions. CO_2 emissions were determined for samples that received urea (i.e., molar urea-to-calcium ratio of 1:0, 1:0.2, 1:1 and 1:2), while control (0:0) and abiotic (NaOH) samples showed CO_2 fluxes near 0. Variation of CO_2 in the vial headspace during incubations was found in

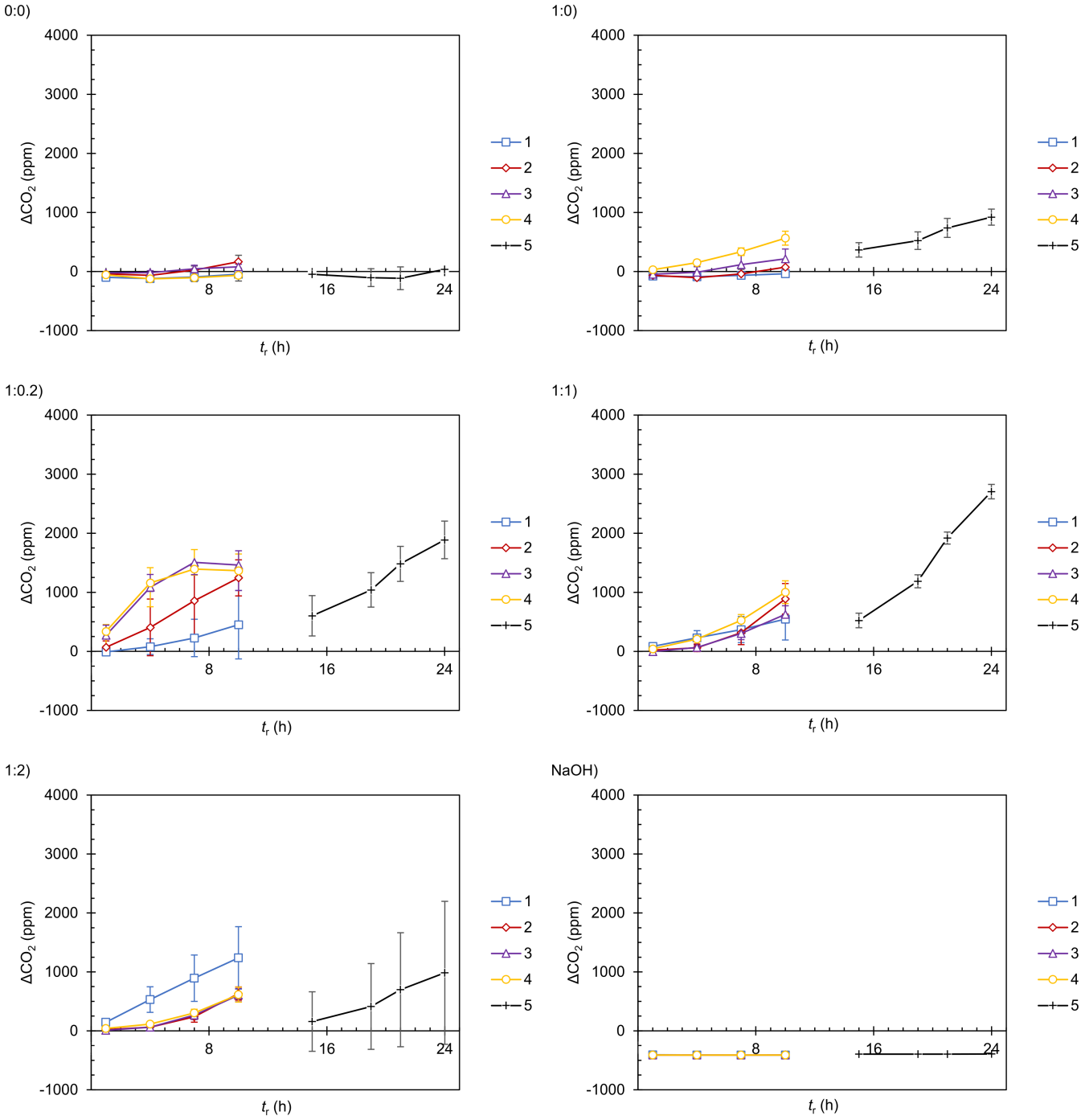

FIGURE 3 Comparison of CO_2 (ppm) evolution in the vial headspace during MICP over five 24 h turnaround incubation for the treatments with solutions with different urea-to-calcium ratios: distilled water (0:0); urea-to-calcium molar ratio of 1:0; 1:0.2; 1:1; 1:2; and distilled water with adjusted pH of 9.5 with NaOH (NaOH). Incubations after solution additions 1, 2, 3, and 4 were run between 0 and 10 h, and from 14 to 24 h after solution addition 5. A total of four gas measurements were performed during every 10 h incubation period at times $t = 1$, 3, 7 and 10 h since vial closure. Gas concentrations are the difference between measured average concentrations and atmospheric concentration at t = 0. Markers and error bars indicate the average and standard deviation of three replicate samples.

each treatment, but not for control samples (Figure 3, '0:0'), indicating soil-atmosphere CO_2 fluxes did not occur. Samples that received NaOH, instead showed negative CO_2 values at $t_r = 1$ h, equivalent to a complete removal of CO_2 from the vial headspace (Figure 3, 'NaOH') and a negative flux of −2.8 μg of CO_2–C h^{-1} g^{-1} soil. Thereafter, CO_2 levels remained stable, hence explaining the CO_2 fluxes close to zero in Figure 2. CH_4 and N_2O fluxes were detected at very low levels (<0.01 μg h^{-1} g^{-1} dry soil) with insignificant variation in concentration in the vial headspace (Figures S3 and S4), indicating fluxes of these gases during MICP did not occur for any case scenario.

Samples that received urea and Ca^{2+} at various proportions showed CO_2 emissions ranging between 0.52 and 4.08 μg of CO_2–C h^{-1} g^{-1} soil (Figure 2). The CO_2 flux dynamics varied with the amount of Ca^{2+} in solution and increasing applications of cementation solution. For samples that did not receive Ca^{2+} (1:0), CO_2 emissions increased slowly but progressively from 0.05 ± 0.11 to 0.62 ± 0.26 μg of CO_2–C h^{-1} g^{-1} soil (Figure 2). With the highest urea-to-calcium ratio (1:0.2), CO_2 fluxes increased markedly from 0.53 ± 1.19 to 4.08 ± 0.84 μg of CO_2–C h^{-1} g^{-1} soil between the first and third incubations and plateaued during the third and fourth incubation period. With equimolar urea-to-calcium ratio (1:1), CO_2 fluxes increased between the first and second incubation period but remained stable in subsequent incubation periods at 0.94 ± 0.19 μg of CO_2–C h^{-1} g^{-1} soil. When Ca^{2+} was twice as high as urea (1:2), CO_2 fluxes were higher in the first incubation and remained lower and stable in following incubations at 0.68 ± 0.01 μg of CO_2–C h^{-1} g^{-1} soil.

During incubations, CO_2 concentration in the vial headspace increased linearly with reaction time (Figure 3, cf. Table S3 for R^2 values). During the third and fourth incubation periods, however, 1:0.2 samples showed a rapid increase in CO_2 between $t_r = 1$ and 7 h, followed by a plateau between $t_r = 7$ and 10 h (Figure 3, '1:0.2'), a pattern that was not observed for any other treatment. With increasing applications of cementation solutions, higher accumulation of CO_2 in the vial headspace was recorded for 1:0 and 1:0.2 samples, while for 1:1 and 1:2 samples the variation in headspace CO_2 was similar, except for the 1:2 samples that showed significantly higher CO_2 in the vial headspace during the first compared to the subsequent incubation periods (Figure 3, '1:2').

Interestingly, CO_2 emissions were lowest when Ca^{2+} was not present (1:0) and highest with the highest urea-to-calcium ratio (1:0.2). The highest CO_2 emissions were recorded for 1:0.2 samples during the third and fourth treatment applications ($t = 48$ to 82 h), with CO_2 emissions two times higher (~4 μg of CO_2–C g^{-1} soil h^{-1}) than for 1:1 and 1:2 samples (<2 μg of CO_2–C h^{-1} g^{-1} soil), and up to four times higher than 1:0 samples (<1 μg CO_2–C h^{-1} g^{-1} soil). Figure 4 presents a comparison of CO_2 in the vial headspace across treatments. During the first treatment application, evolved CO_2 in the vial headspace was higher with higher Ca^{2+} content (1:2 > 1:1 ~ 1:0.2) (Figure 4, '1'). Instead, from the second to the fourth treatment applications, CO_2 in the headspace was consistently higher with lower Ca^{2+} content (1:0.2 > 1:1 ~ 1:2) (Figure 4, '2' to '4'). Remarkably, without Ca^{2+} (1:0), CO_2 increase in the vial headspace remained near zero the first two treatment applications, showing a clear accumulation of CO_2 in the vial headspace only from the third application of cementation solution onwards, then reaching similar values to the 1:2 samples during the fourth treatment application.

Observations from the second half of the 24 h reaction time during the fifth treatment application indicated that CO_2 in the vial headspace continued to increase with reaction time for all treatments containing urea (Figure 3). CO_2 accumulation in the vial headspace was highest for the equimolar urea-to-calcium ratio (1:1), followed by the highest (1:0.2) and lowest (1:2) urea-to-calcium ratios, respectively (Figure 4). Equimolar urea-to-calcium ratio (1:1), double calcium compared to urea (1:2) and samples that did not receive Ca^{2+} (1:0) showed higher CO_2 emissions compared to incubations conducted during the first 10 h of reaction time (first to fourth treatment applications) (2.51 ± 0.41, 1.44 ± 0.77 and 0.65 ± 0.51 μg CO_2–C g^{-1} soil h^{-1}, respectively), while the treatment containing the highest urea-to-calcium ratio (1:0.2) showed a marked decrease in CO_2 fluxes (1.48 ± 1.11 μg CO_2–C g^{-1} soil h^{-1}) compared to the initial 10 h reaction time of the third and fourth treatment applications (Figure 2).

Estimated cumulative CO_2–C emissions during MICP at various urea-to-calcium ratios over 10-h incubation periods based on average fluxes (Figure 2) are presented in Figure 5. Despite the different observed dynamics, the equimolar urea-to-calcium ratio (1:1) and the double Ca^{2+} (1:2) treatments showed similar cumulative CO_2 emissions (47 to 58 μg CO_2–C g^{-1} soil), two to three times higher than the treatment without Ca^{2+} (1:0) (~18 μg CO_2–C g^{-1} soil). The treatment with the highest urea-to-calcium ratio (1:0.2) emitted roughly two times the amount of CO_2 (112 μg CO_2–C g^{-1} soil) compared to the 1:1 and 1:2 samples, and five to six times to samples that did not receive Ca^{2+} (1:0).

3.4 | Soil total inorganic carbon

An increase in soil TIC occurred only in treatments containing urea and Ca^{2+} (Figure 6). The initial soil TIC content was 3.2 μg C g^{-1} of dry soil and increased

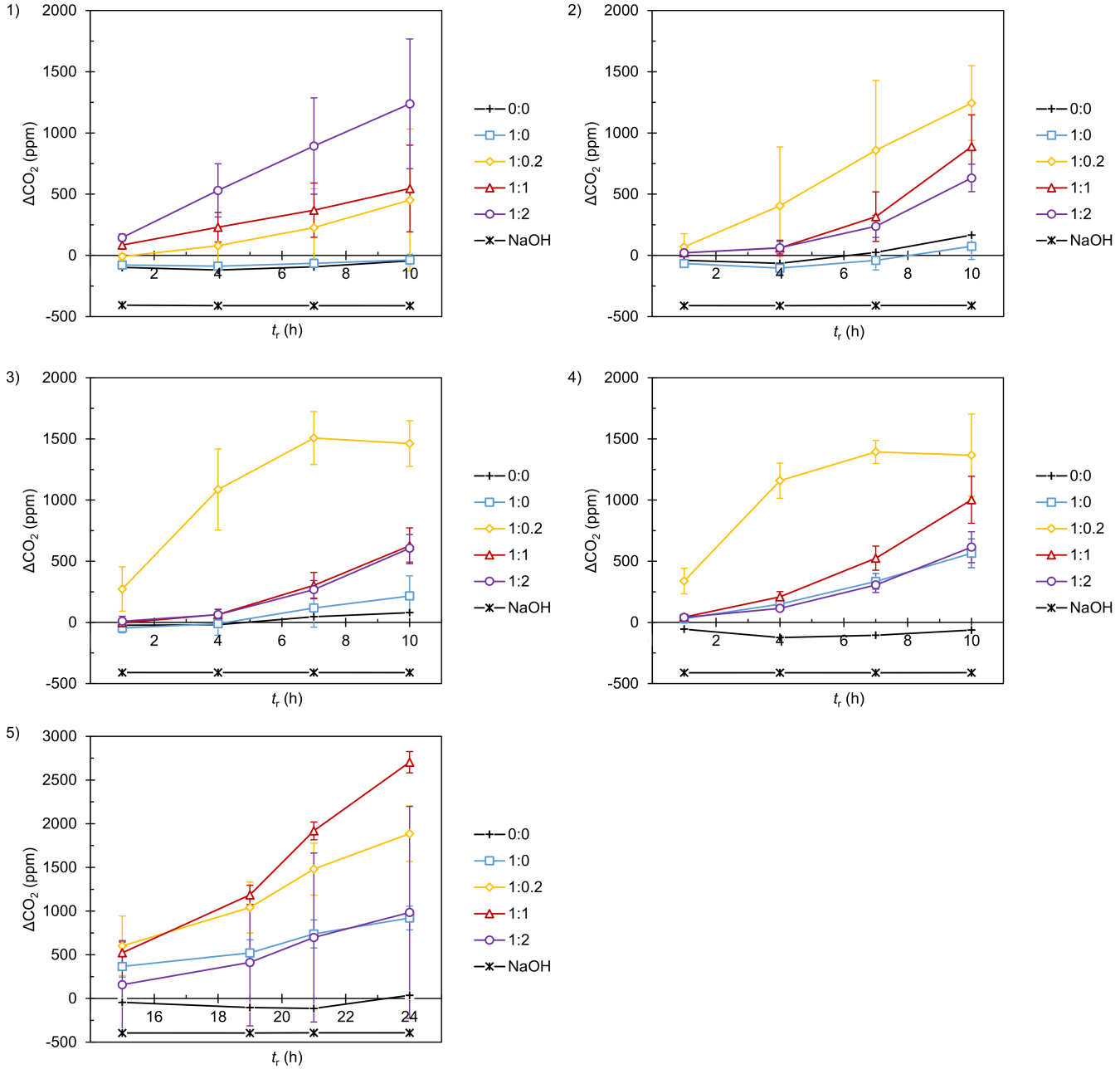

FIGURE 4 Comparison of CO_2 (ppm) evolution in vial headspace during MICP over 10 h incubation for solution treatments: distilled water (0:0); urea-to-calcium molar ratio of 1:0; 1:0.2; 1:1; 1:2; and distilled water with adjusted pH of 9.5 with NaOH (NaOH), over five incubation periods (1–5). Incubation time (1) to (4) t = 0–10 h and of 5) t = 14 h to 24 h. Four gas measurements were performed during every 10 h incubation period at t = 1, 3, 7 and 10 h since vial closure. Gas concentrations are the difference between measured average concentrations and atmospheric concentration at t = 0. Markers and error bars indicate the average and standard deviation of three replicate samples.

drastically during the five cementation periods to values between 1135 and 1470 μg C g^{-1} of dry soil. Significant differences in precipitated TIC across treatments containing Ca^{2+} were not observed. On average, a urea-to-calcium ratio of 1:1 was associated with the largest TIC accumulation in soil, followed by the 1:0.2 and 1:2 treatments (1470 ± 531, 1217 ± 198 and 1136 ± 336 μg C g^{-1} dry soil, respectively).

3.5 | Isotopic composition of precipitated and emitted carbon

The isotopic composition of precipitated $CaCO_3$ in treatments containing urea and Ca^{2+} was similar for all treatments, with an average $\delta^{13}C_{TIC}$ of −40.7 ± 0.8‰ and $\delta^{18}O_{TIC}$ of −14.7 ± 1.0‰ (Figure 7), indicating the origin of precipitated carbon was urea (Table S2). Soil samples

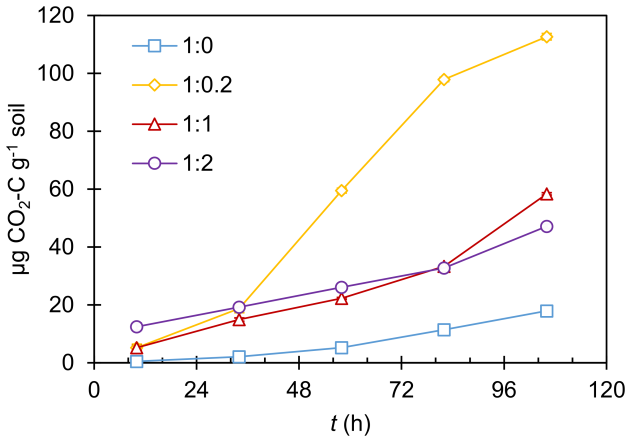

FIGURE 5 Cumulative CO_2–C emitted during MICP at urea-to-calcium molar ratios of 1:0, 1:0.2, 1:1 and 1:2 estimated from average CO_2–C fluxes over 10 h incubation periods in Figure 2.

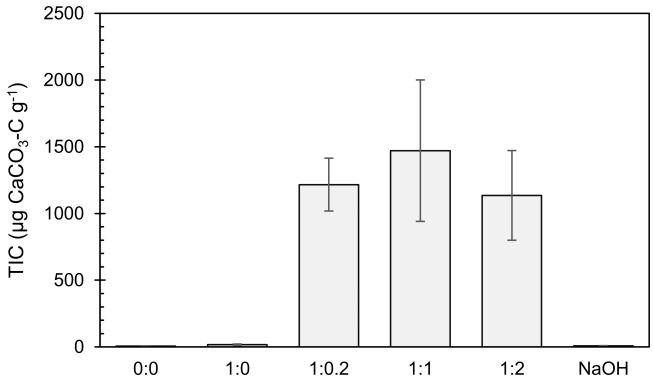

FIGURE 6 Soil total inorganic carbon at the end of MICP treatments of varying urea-to-calcium molar ratios (1:0, 1:0.2, 1:1 and 1:2), distilled water (0:0, control) and solution of adjusted pH of 9.5 with sodium hydroxide (NaOH) determined by gas chromatography–continuous flow–isotope ratio mass spectrometry. Bars and error bars indicate the average and standard deviation of three replicate samples.

treated with distilled water (0:0), the alkaline pH solution (NaOH) and urea without Ca^{2+} (1:0) showed a similar isotopic signature to the untreated soil (Table S1). Further, the isotopic composition of evolved CO_2 in the vials' headspace during MICP across treatments was $\delta^{13}C_{CO2} = -48.0 \pm 3.3‰$, indicating that the source of the emitted CO_2 was mainly urea for all treatments with urea (Figure 8).

3.6 | Carbon mass balance

The carbon applied to vials in a single incubation estimated from the mass of chemical compounds added and known concentration of carbon in each compound (Table S2) was 8617 μg C g^{-1} dry soil, and the total carbon applied 43,068 μg C g^{-1} dry soil (for further detail see Tables S6–S8). Based on the cumulative CO_2–C emitted (Figure 5) and precipitated $CaCO_3$–C (Figure 6), emitted and precipitated carbon were estimated to account for <0.35% and <4.5% of the total carbon applied, while >95% of the total carbon applied remained unaccounted for (Table S9), suggesting it remained in solution and/or taken up by microbial biomass. Urea-C represented 60% of the total carbon applied (Table S8). If both emitted and precipitated carbon were solely of urea origin (based on results of Section 3.5), the data suggest that between 5.9 to 7.6% of the total urea-C introduced was emitted and/or precipitated. Based on the soil TIC data (Figure 6), the equivalent amount of precipitated Ca^{2+} was calculated assuming precipitated carbonates were pure $CaCO_3$. The ratio of total applied Ca^{2+} in the Ca^{2+} treatments to the Ca^{2+} precipitated as $CaCO_3$ revealed that 91.5% of introduced Ca^{2+} was precipitated in the 1:0.2 treatment, while the ratio decreased to 22 and 8.5% in the 1:1 and 1:2 urea-to-calcium treatments, respectively (Table S9).

4 | DISCUSSION

4.1 | Main results

Our study on GHG fluxes during biostimulation of MICP in a quartz sand revealed CO_2 emissions, but no indication of N_2O and CH_4 fluxes (Figure 2). The results of this study demonstrate that varying the urea-to-calcium ratio in solution influenced CO_2 flux dynamics, solution pH and the extent of carbonate precipitation. Overall, we observed that for reaction times of 10 h, increasing Ca^{2+} concentration in treatment solution from 20 to 200 mM decreased cumulative CO_2 emissions (Figure 5), rendered lower solution pH (Figure 1), and produced a similar amount of precipitated carbonates in soil (Figure 6).

4.2 | GHG fluxes

CO_2 emissions in this study are in line with CO_2 emissions derived from MICP on the same soil observed by Casas et al. (2020). In Casas et al. (2020), urea and Ca^{2+} concentrations in treatment solution were 100 and 20 mM, respectively, just as the highest urea-to-calcium ratio (1:0.2) treatment used in this study. Average CO_2 emissions of eight cementation treatments of 24 h reaction time were reported to be 1.33 ± 0.44 g CO_2–C m^{-2}, equivalent to 0.58 ± 0.19 μg CO_2–C h^{-1} g^{-1} soil, and to increase linearly during reaction time. In this study,

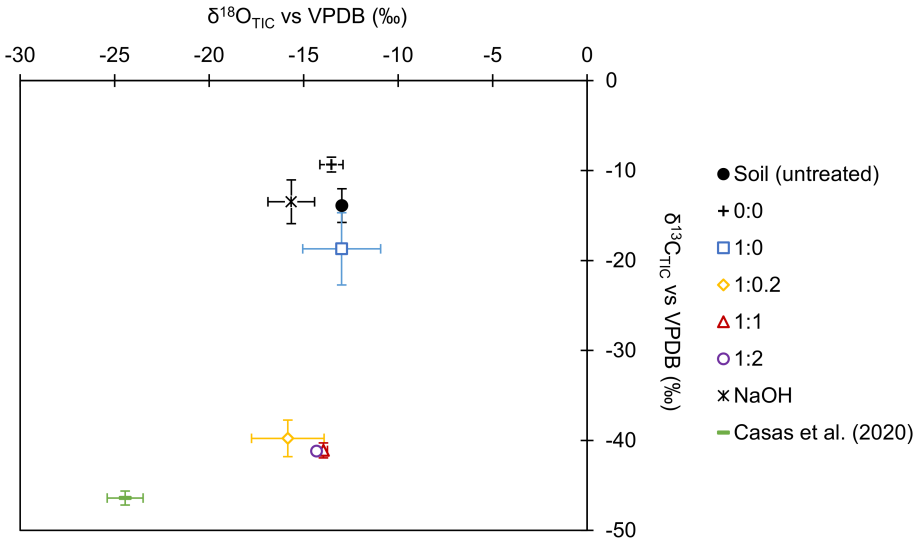

FIGURE 7 Carbon and oxygen isotopic signatures of precipitated carbonates in soil prior to treatment (Soil, untreated), following end of treatment with distilled water (0:0, control), MICP solution of varying urea-to-calcium molar ratio (1:0, 1:0.2, 1:1 and 1:2), and solution of adjusted pH of 9.5 with sodium hydroxide (NaOH) determined by gas chromatography–continuous flow–isotope ratio mass spectrometry. Additionally, the graph includes results of the isotopic composition of MICP at equimolar urea-to-calcium ratio of Casas et al. (2020) on the same soil for comparison. Markers and error bars indicate the average and standard deviation of three replicate samples.

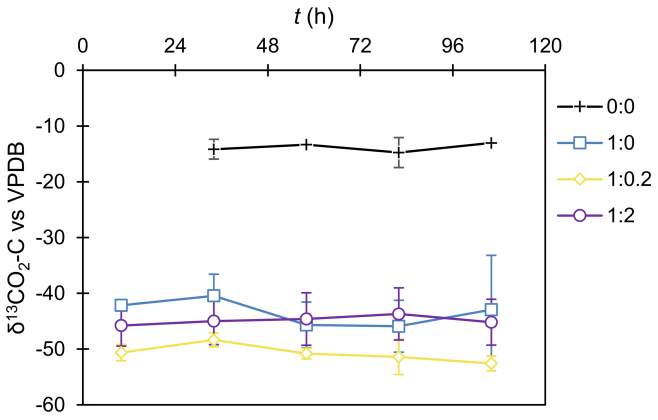

FIGURE 8 Carbon isotopic signature of CO_2 evolved in the vial headspace at the end of 10 h incubation periods of quartz sand treated with distilled water (0:0, control) and MICP solution of varying urea-to-calcium molar ratios (1:0, 1:0.2, 1:1, and 1:2) determined by gas chromatography–continuous flow–isotope ratio mass spectrometry. Markers and error bars indicate the average and standard deviation of three replicate samples.

average CO_2 emissions of the 1:0.2 treatment increased from 0.53 ± 1.19 to 4.08 ± 0.84 μg of CO_2–C h^{-1} g^{-1} soil, linearly between the first and third incubations, plateauing during the third and fourth incubation, and dropping for reaction time longer than 10 h period. While results of the first incubation period are comparable with the results obtained by Casas et al. (2020), CO_2 emissions of subsequent incubations determined in this study are significantly higher. CO_2 concentration in Casas et al. (2020) were recorded with a soil chamber system (LI-8100, LI-COR Biosciences, LICOR Inc., United States) every hour for 10 min at a frequency of 1 s^{-1} by closing a 3 kg soil column which otherwise was open to the atmosphere, while in this study vials remained closed throughout the entire incubation, the mass of soil was 1.5 g and the measuring frequency was four times every 10 h. While the cause of discrepancy could be partially due to the different experiment conditions and measuring devices, the main cause remains unclear. CO_2 emissions of MICP in aqueous samples obtained from travertine environments have also been reported by Okyay et al. (2016) where both CO_2 emissions and sequestration were observed in incubation experiments and attributed to MICP either acting as a source or a sink of CO_2 depending on bacterial community composition.

N_2O fluxes are likely to occur in MICP due to the abundance of NH_4^+. N_2O is a minor product of both nitrification and denitrification (Stein & Nicol, 2018). Ammonia oxidation in quartz sand was observed after 27 days of being in contact with treatment solution (Gat et al., 2016), and a later study indicated an increase in activity of nitrifying bacteria and/or archaea during MICP (Tsesarsky et al., 2016). However, nitrite (NO_2^-) and nitrate (NO_3^-) were found at very low concentrations to below limit of detection in a previous MICP experiment on the same soil as used in this study during and 29 days following end of MICP treatment, indicating nitrification did not occur (Casas et al., 2020). Environmental factors influencing the nitrification process are

substrate availability, soil matrix (e.g., clay content), water status, oxygen availability, temperature, salinity and pH (Norton, 2011; Sahrawat, 2008). In particular, nitrifying bacteria require molecular oxygen as electron acceptors. Oxygen availability is hindered in water saturated conditions thus reducing nitrification rates. Nitrification is observed at pH between 6 and 10 however, nitrifiers are sensitive to free NH_3, which is exacerbated by alkaline pH and high concentration of NH_4^+ (Breuillin-Sessoms et al., 2017; Kim et al., 2006; Venterea et al., 2015). Nitrifying bacteria are chemolithotrophs, thus grow in media containing mineral salts, where magnesium and phosphate, despite at very low concentrations, were determined essential (Meiklejohn, 1952). Key enzymes involved in nitrification include ammonia monooxygenase, hydroxylamine dehydrogenase and nitrite oxidoreductase, the former containing iron/copper and the latter requiring molybdenum as cofactor (Stein & Nicol, 2018). While the reason for the observed results with respect to N_2O emissions remains unclear, it is plausible that a lack of oxygen combined with free NH_3 could have inhibited nitrification during MICP. Additionally, it could be that elements required for enzyme synthesis were a limiting factor. In any case, despite the results of our study indicating that nitrification may not occur during MICP, additional studies are necessary to test whether these observations hold over time when excess ammonia degasses from the system, whether inhibition is related to nutritional requirements, lack of oxygen, presence of essential elements, or other factors.

4.3 | CO_2 flux dynamics

The dynamics of CO_2 fluxes during MICP at varying Ca^{2+} concentrations were complex. CO_2 emissions were lowest without Ca^{2+} (1:0) and highest with the lowest Ca^{2+} concentration (1:0.2), while increasing Ca^{2+} resulted in lower CO_2 emissions (Figure 2). Urease enzyme reaction kinetics are affected by pH, such that its affinity for urea decreases with decreasing pH, but reaction rates are higher at circumneutral pH and decrease with increasing pH (Cabrera et al., 1991; Stocks-Fischer et al., 1999). With higher urea hydrolysis reaction rates, more CO_2 is produced in the same period of time and thus can potentially be emitted. Treatments that contained Ca^{2+} (1:0.2, 1:1 and 1:2) resulted in lower solution pH compared to the treatment that excluded Ca^{2+} (1:0) (Figure 1), which may have resulted in increased enzyme activity (i.e., production of CO_2) and therefore result in higher CO_2 emissions, explaining the observed higher CO_2 emissions obtained when Ca^{2+} was present. On the other hand, the high pH induced by the treatment that excluded Ca^{2+} (1:0, pH = 9) may have acted as a sink of atmospheric CO_2 and partially balanced CO_2 emissions produced by urea hydrolysis, particularly during the initial treatment applications (Figure 3). In abiotic experiments with various MICP treatment media, Okyay and Rodrigues (2015) observed CO_2 sequestration by the alkaline treatment solutions where pH had been adjusted to the alkaline pH achieved by urea hydrolysis using that same media. In this study, complete CO_2 removal from the vial headspace was evident in the NaOH treatment (Figure 3), which was accompanied by a reduction in pH of 0.5 units (Figure 1). Urea hydrolysis by the treatment that contained solely urea (1:0) induced a similar pH compared to the NaOH treatment (Figure 1). This demonstrated that abiotic CO_2 sequestration was taking place due to solution alkalinity, contributing to the lower CO_2 emissions observed with the treatment without Ca^{2+}.

Based on the effect of pH on both urease activity and abiotic CO_2 sequestration, the lowest CO_2 emissions in treatments containing Ca^{2+} should have been observed for the treatment that contained the lowest Ca^{2+} content (i.e., 1:0.2). Instead, cumulative CO_2 emissions were higher (Figure 5) for the treatment that induced the highest pH (Figure 1) (i.e., 1:0.2), indicating that pH could not solely explain the observed results. Urease activity can be negatively affected by Ca^{2+} content, implying that the higher the Ca^{2+} concentration, the stronger is the inhibitory effect. A recent study on urease activity under varying Ca^{2+} concentrations reported no inhibition to complete inhibition of urease activity at Ca^{2+} concentrations <10 mM and >200 mM, respectively (Cui et al., 2022). The carbon and Ca^{2+} mass balances of our study indirectly indicated a lower amount of urea hydrolysed with increasing Ca^{2+}, supporting the results of Cui et al. (2022). Thus, presumably, increasing Ca^{2+} concentrations from 20 to 200 mM may have increasingly inhibited urease activity, resulting in less CO_2 produced by urea hydrolysis and lower CO_2 emissions.

4.4 | Sources of CO_2 emissions

In MICP, potential sources of CO_2 emissions originate from the breakdown of urea into CO_2 and NH_3, and additional microbial respiration through the breakdown of other organic carbon sources present both in treatment solution (e.g., molasses, sodium acetate) and soil (e.g., humus). The soil used in this study had very low carbon content (TOC = 0.02%, TIC = 0.0003%, Table S1), hence sources of CO_2 emissions could be assumed to originate predominantly from the treatment solution. The similarity in isotopic signature of evolved CO_2

(−48.0 ± 3.3‰, Figure 8) with urea-C (−41.03 ± 0.12%, Table S2) proved that the evolved CO_2 was of urea origin and the contribution of other carbon sources was small. In line with results of this study, experiments conducted on agricultural soils amended with synthetic urine containing $\delta^{13}C$ labelled urea indicated urea-C was the main contributor to CO_2 emissions the first 2 days after application but declined rapidly from day three onwards (Ambus et al., 2007).

4.5 | Sources of CO_2 precipitation

CO_2 sequestration in MICP can occur due to CO_2 precipitation as Ca^{2+} carbonate minerals (mineral trapping) and CO_2 storage in solution due to an increase in solution pH resulting from urea hydrolysis, which consumes protons from the soil solution due to conversion of NH_3 to NH_4^+ (solubility trapping). With an increase in solution pH, atmospheric CO_2 is drawn into the solution to neutralise excess OH^-. In the absence of soil organic matter, sources of CO_2 for MICP may thus originate from atmospheric CO_2, dissolved inorganic carbon (DIC) from minerals (e.g., carbonates) or CO_2 produced by microbial respiration (Okyay et al., 2016). In this study, MICP was indicated by the increase in soil TIC in samples that received urea and Ca^{2+}, as opposed to samples that did not receive Ca^{2+}, where increase in soil TIC was not observed (Figure 6). The similarity in isotopic C composition of precipitated carbonates (−40.7 ± 0.8‰, Figure 7) and urea-C (−41.03 ± 0.12%, Table S2) indicated that precipitated carbon was of urea origin, in line with previous observations by Millo et al. (2012) and Casas et al. (2020).

4.6 | Changes in pH during MICP

During urea hydrolysis, there are two main processes which alter pH, namely the protonation of NH_3 molecules released by urea hydrolysis, and the change in speciation of dissolved CO_2. NH_3 molecules undergo protonation with hydrogen (H^+) from water to produce ammonium (NH_4^+) and hydroxide ions (OH^-), thus increasing pH. CO_2 molecules dissolved in water produce carbonic acid (H_2CO_3), which deprotonates to bicarbonate (HCO_3^-) and carbonates (CO_3^{2-}), releasing one and two H^+, respectively, decreasing solution pH. For every mole of urea hydrolysed, 2 moles of NH_3 and 1 mole of CO_2 are produced. Below a pH of 8.5, HCO_3^- is the dominant speciation of CO_2 in solution, so that only 1 mole of H^+ will be produced. Therefore, two OH^- moles are produced for every mole of H^+, resulting in a net solution pH increase of up to 9, when NH_4^+ begins to deprotonate to NH_3 and degas from the soil-solution system. The results of the treatment solution without Ca^{2+} (1:0) are in agreement with the latter, where a net increase in pH to 9 occurred followed by stabilisation (Figure 1). With the addition of Ca^{2+}, $CaCO_3$ minerals can form, with favourable conditions for precipitation above pH of 8.5. As HCO_3^- deprotonates to CO_3^{2-}, an additional mole of H^+ is released, such that the 2 moles of OH^- initially produced by NH_3 protonation are balanced, resulting in a decrease in pH and stabilisation of pH around 8.25, which is the pH of pure $CaCO_3$ solution (Bache, 1984). In this study, when Ca^{2+} was introduced to the system, the initially higher pH and decreasing trend with increasing reaction time (Figure 1) were consistent with initial rapid increase in solution pH due to urea hydrolysis and subsequent decrease due to $CaCO_3$ precipitation (Dupraz et al., 2009).

4.7 | Effect of increasing the Ca^{2+} concentration on pH

pH stabilised at lower values with increasing Ca^{2+} concentration (i.e., approx. 8, 7.5 and 7.3 for urea-to-calcium molar ratios 1:0.2, 1:1 and 1:2, respectively) (Figure 1) than the earlier reported pH values of MICP in solution (pH = 8–8.7 for a treatment solution containing 20 mM Ca^{2+} and 333 mM urea) (Dupraz et al., 2009). $CaCl_2$ produces slightly acidic solutions (salt of a weak base and a strong acid), which may have partly contributed to the observed lower pH with increasing $CaCl_2$. Additionally, release of protons from the adsorber matrix of the soil being exchanged with Ca^{2+} likely contributed to further lowering of the pH (Bache, 1974; Houba et al., 2000). For urea-to-calcium molar ratios of 1:1 and 1:2 (containing 100 and 200 mM Ca^{2+}, respectively), values were similar to pH values of $CaCO_3$ dominated soils (pH = 7.5) (Bache et al. 1984).

4.8 | Effect of Ca^{2+} concentration on the TIC

Contrary to what was hypothesised, increasing Ca^{2+} in solution from 20 to 200 mM did not result in increased $CaCO_3$ precipitation and resulted in similar soil TIC values (Figure 6). The fact that the total amount of TIC was not significantly different between the 1:0.2, the 1:1 and the 1:2 treatments (Figure 6) indicated that Ca^{2+} was not a limiting factor for carbonate formation but instead it was the concentration of CO_3^{2-} in the soil solution. This was likely related to the inhibitory effect of Ca^{2+} on urease activity, which induced lower CO_2

availability for carbonation, and pH ≤8, which limited the extent to which carbonation could occur.

4.9 | Mechanisms for observed CO_2 emissions/sequestration

During MICP, the $CO_2(g) \leftrightarrow CO_2(aq) \leftrightarrow H_2CO_3(aq) \leftrightarrow HCO_3^-(aq) \leftrightarrow CO_3^{2-}(aq) \leftrightarrow CO_3^{2-}(s)$ equilibrium in a system is disequilibrated by production of additional CO_2 from urea hydrolysis. The precipitation of calcium carbonate in MICP occurs extracellularly. That and the increase in NH_4, DIC and pH in soil-solution necessarily imply that NH_3 and CO_2 from urea are to some extent excreted outside the cell. Once inorganic carbon is in the outer cell environment, its speciation is dependent on the total inorganic carbon in the system, solution pH and CO_2 partial pressure in the air-filled pore space of the soil and ultimately in the headspace of the GC vials. With increasing pH and CO_2 partial pressure, the liquid phase has more capacity to store inorganic carbon and vice versa, while the total carbon in the system determines whether there is sufficient inorganic carbon in the system for it to be quantifiable in all its possible speciation forms and phases. CO_2 gas measurements with the NaOH treatment (Figure 4), where no carbon was applied to the system, evidenced the effect of pH on CO_2 solubility trapping, where atmospheric CO_2 entered the solution due to alkaline pH inducing a decrease with respect to initial solution pH (Figure 1) and quantifiable CO_2 in the headspace was negligible due to limited total carbon in the system (Figure 4). When urea but no Ca^{2+} were present (1:0 treatment), CO_2 gas measurements near zero indicated that the CO_2 produced via urea hydrolysis mostly accumulated in solution (Figure 4) due to solubility trapping, as indicated by the increase in solution pH to 9 (Figure 1). However, as microbial activity increased with repeated treatment applications (i.e., more CO_2 was produced), solubility trapping could not balance the amount of CO_2 produced from urea hydrolysis, resulting in an accumulation of CO_2 in the vial headspace/CO_2 emissions. Several interconnected factors might explain the varying CO_2 emissions observed when Ca^{2+} was introduced at varying urea-to-calcium ratios. On the one hand, increasing Ca^{2+} in solution and precipitation of calcium carbonate decreased solution pH (Figure 1), resulting in less capacity of the solution to store carbon and higher accumulation of CO_2 in the vial headspace. On the other hand, slower urea hydrolysis rates with increasing Ca^{2+} directly resulted in a lower amount of CO_2 in the system, which would explain the lower accumulation of CO_2 in the vial headspace observed with increasing Ca^{2+}. Finally, limited urea hydrolysis and insufficient increase in solution pH to reach favourable conditions for calcium carbonate precipitation (pH >8.5) resulted in similar calcium carbonate precipitation across treatments including urea and Ca^{2+}. Accumulation of CO_2 in the vial headspace observed in this study thus reflected an increase in dissolved CO_2 produced from urea hydrolysis that could not be balanced by increased capacity to store CO_2 in solution provided by increase in pH (solubility trapping) and storage of CO_2 as solid in calcium carbonate (mineral trapping).

4.10 | Chemical efficiency

Finally, it is worth highlighting that CO_2–C emissions and precipitated $CaCO_3$-C accounted for less than 0.35% and <4.5%, respectively, of the total applied carbon (Table S9). This indicated that the amount of precipitated carbon was about tenfold higher than emitted carbon. Furthermore, the Ca^{2+} precipitated represented 91, 22 and 8.5% of applied Ca^{2+} for treatment solutions containing 20, 100 and 200 mM, respectively. These results further indicate a small amount of urea was hydrolysed and highlight a very low efficiency of usage of applied chemicals, and that longer reaction times were necessary for full degradation of urea. Reaction times of 8 to 10 h have been reported optimum for complete urea hydrolysis in bioaugmentation experiments on quartz sand with *S. pasteurii* (Al Qabany et al., 2012). While different bacteria express different urea hydrolysis rates, experiments on biostimulation vs bioaugmentation showed similar overall urea hydrolysis rates (Gomez et al., 2019). This highlights that reaction time of MICP in soil via biostimulation should be adjusted to specific soil bulk urea hydrolysis rates and Ca^{2+} concentration.

5 | CONCLUSIONS

Our study on GHG fluxes during biostimulation of MICP on a quartz sand indicated MICP was a source of CO_2 emissions, while no N_2O nor CH_4 was produced during MICP treatment. Varying the relative proportion of Ca^{2+} with respect to urea-C had an effect on CO_2 emissions, soil-solution pH, and the extent of carbonate precipitation in soil. Increasing the Ca^{2+} concentration from 20 to 200 mM had an inhibitory effect on urease activity, such that less CO_2 and NH_4^+ were produced. On the one hand, the lower production of NH_4^+ and increasing exchange of protons from soil with increasing Ca^{2+} concentration resulted in soil solutions of lower pH. On the other hand, the lower production of CO_2 limited availability of carbonates for precipitation and resulted in

lower CO_2 emissions. When urea exceeded Ca^{2+}, $CaCO_3$ precipitation was maximised, but CO_2 emissions were highest. When Ca^{2+} exceeded urea, CO_2 emissions decreased but the extent of $CaCO_3$ precipitation was limited by the availability of CO_3^{2-}, resulting in a low chemical usage efficiency of applied urea and Ca^{+} with respect to precipitated $CaCO_3$. Based on the balance of precipitated carbon and CO_2 emissions, we recommend using treatment solutions of equimolar urea-to-calcium concentrations to reduce overall CO_2 emissions while maintaining the same degree of soil carbonation. However, results suggest that longer reaction times were necessary with increasing Ca^{2+} with respect to urea, and additional studies are required to compare emitted and precipitated CO_2 at similar amounts of urea hydrolysed. During reaction time, urea was the main source of precipitated and emitted CO_2. Results further indicate that the abiotic CO_2 sequestration mechanism by the highly alkaline solution pH induced by urea hydrolysis was relevant in balancing CO_2 emissions at pH of 9. The results of this study are expected to serve as a benchmark for future studies on CO_2 fluxes of MICP in soils (e.g., varying reaction time, urea concentration, soil type, soil organic matter content) and inform life cycle assessment of MICP to quantify the environmental impact of the technique.

AUTHOR CONTRIBUTIONS

Carla Comadran-Casas: Conceptualization; data curation; formal analysis; funding acquisition; investigation; methodology; resources; writing – original draft. **Nicolas Brüggemann:** Conceptualization; methodology; resources; supervision; writing – review and editing. **M. Ehsan Jorat:** Conceptualization; funding acquisition; resources; project administration; supervision; writing – review and editing.

ACKNOWLEDGEMENTS

Special thanks are given to the funding bodies, the laboratory technicians F. Leistner, H. Wissel, S. Kummer, and L. Weihermüller of the Institute of Bio- and Geosciences, Agrosphere (IBG-3), Forschungszentrum Jülich for their expertise and carrying out analysis of samples, and the managers of Barrasford quarry, S. Bell, and Quarzweke Frechen quarry, A. Graf, for sourcing the materials used in this study. Further thanks are given to Dr Alexander Graf for his continuous support and involvement in this work. For the purpose of open access, the author has applied a Creative Commons Attribution (CC BY) licence to any Author Accepted Manuscript version arising from this submission.

FUNDING INFORMATION

This research was conducted with the financial support of the Scottish Alliance for Geoscience, Environment and Society (SAGES, www.sages.ac.uk), the Research-led Innovation Nodes for Contemporary Society (Rlincs) programme of Abertay University, the Norman Fraser Design Trust, the Institute of Bio- and Geosciences, Agrosphere (IBG-3), Forschungszentrum Jülich and the SAGES 5th Small Grant Scheme (https://www.sages.ac.uk/graduate-school/small-grantsscheme/) in a collaborative framework between SAGES and ABC/J Geoverbund (www.geoverbund.de) partner organisations.

DATA AVAILABILITY STATEMENT

The datasets generated for this study are available upon request from the corresponding author.

ORCID

Carla Comadran-Casas https://orcid.org/0000-0003-0728-4395

REFERENCES

Al Qabany, A., Soga, K., & Santamarina, C. (2012). Factors affecting efficiency of microbially induced calcite precipitation. *Journal of Geotechnical and Geoenvironmental Engineering*, *138*(8), 992–1001. https://doi.org/10.1061/(ASCE)GT.1943-5606.0000666

Ambus, P., Petersen, S. O., & Soussana, J. F. (2007). Short-term carbon and nitrogen cycling in urine patches assessed by combined carbon-13 and nitrogen-15 labelling. *Agriculture, Ecosystems & Environment*, *121*(1–2), 84–92. https://doi.org/10.1016/j.agee.2006.12.007

Bache, B. W. (1974). Soluble aluminium and calcium-aluminium exchange in relation to the pH of dilute calcium chloride suspensions of acid soils. *Journal of Soil Science*, *25*(3), 320–332. https://doi.org/10.1111/j.1365-2389.1974.tb01128.x

Bache, B. W. (1984). The role of calcium in buffering soils. *Plant, Cell & Environment*, *7*(6), 391–395. https://doi.org/10.1111/j.1365-3040.1984.tb01428.x

Benhelal, E., Zahedi, G., Shamsaei, E., & Bahadori, A. (2013). Global strategies and potentials to curb CO_2 emissions in cement industry. *Journal of Cleaner Production*, *51*, 142–161. https://doi.org/10.1016/j.jclepro.2012.10.049

Breuillin-Sessoms, F., Venterea, R. T., Sadowsky, M. J., Coulter, J. A., Clough, T. J., & Wang, P. (2017). Nitrification gene ratio and free ammonia explain nitrite and nitrous oxide production in urea-amended soils. *Soil Biology and Biochemistry*, *111*, 143–153. https://doi.org/10.1016/j.soilbio.2017.04.007

Cabrera, M. L., Kissel, D. E., & Bock, B. R. (1991). Urea hydrolysis in soil: Effects of urea concentration and soil pH. *Soil Biology and Biochemistry*, *23*(12), 1121–1124. https://doi.org/10.1016/0038-0717(91)90023-D

Casas, C. C., Graf, A., Brüggemann, N., Schaschke, C. J., & Jorat, M. E. (2020). Dolerite fines used as a calcium source for microbially induced calcite precipitation reduce the environmental carbon cost in sandy soil. *Frontiers in Microbiology*, *11*, 2181. https://doi.org/10.3389/fmicb.2020.557119

Castro-Alonso, M. J., Montañez-Hernandez, L. E., Sanchez-Muñoz, M. A., Macias Franco, M. R., Narayanasamy, R., & Balagurusamy, N. (2019). Microbially induced calcium carbonate precipitation (MICP) and its potential in bioconcrete:

Microbiological and molecular concepts. *Frontiers in Materials*, *6*, 126. https://doi.org/10.3389/fmats.2019.00126

Chang, I., Im, J., & Cho, G. C. (2016). Introduction of microbial biopolymers in soil treatment for future environmentally-friendly and sustainable geotechnical engineering. *Sustainability*, *8*(3), 251. https://doi.org/10.3390/su8030251

Chang, I., Lee, M., & Cho, G. C. (2019). Global CO_2 emission-related geotechnical engineering hazards and the mission for sustainable geotechnical engineering. *Energies*, *12*(13), 2567. https://doi.org/10.3390/en12132567

Cui, M. J., Teng, A., Chu, J., & Cao, B. (2022). A quantitative, high-throughput urease activity assay for comparison and rapid screening of ureolytic bacteria. *Environmental Research*, *208*, 112738. https://doi.org/10.1016/j.envres.2022.112738

Debajyoti, P., & Skrzypek, G. (2007). Assessment of carbonate-phosphoric acid analytical technique performed using GasBench II in continuous flow isotope ratio mass spectrometry. *International Journal of Mass Spectrometry*, *262*, 180–186. https://doi.org/10.1016/jijms.2006.11.006

DeJong, J. T., Fritzges, M. B., & Nüsslein, K. (2006). Microbially induced cementation to control sand response to undrained shear. *Journal of Geotechnical and Geoenvironmental Engineering*, *132*(11), 1381–1392. https://doi.org/10.1061/(ASCE)1090-0241(2006)132:11(1381)

Deng, X., Li, Y., Liu, H., Zhao, Y., Yang, Y., Xu, X., Cheng, X., & Wit, B. D. (2021). Examining energy consumption and carbon emissions of microbial induced carbonate precipitation using the life cycle assessment method. *Sustainability*, *13*(9), 4856. https://doi.org/10.3390/su13094856

Dupraz, S., Parmentier, M., Ménez, B., & Guyot, F. (2009). Experimental and numerical modeling of bacterially induced pH increase and calcite precipitation in saline aquifers. *Chemical Geology*, *265*(1–2), 44–53. https://doi.org/10.1016/j.chemgeo.2009.05.003

Fang, L., Niu, Q., Cheng, L., Jiang, J., Yu, Y. Y., Chu, J., Achal, V., & You, T. (2021). Ca-mediated alleviation of Cd^{2+} induced toxicity and improved Cd^{2+} biomineralization by Sporosarcina pasteurii. *Science of the Total Environment*, *787*, 147627. https://doi.org/10.1016/j.scitotenv.2021.147627

Fujita, Y., Redden, G. D., Ingram, J. C., Cortez, M. M., Ferris, F. G., & Smith, R. W. (2004). Strontium incorporation into calcite generated by bacterial ureolysis. *Geochimica et Cosmochimica Acta*, *68*(15), 3261–3270. https://doi.org/10.1016/j.gca.2003.12.018

Gat, D., Ronen, Z., & Tsesarsky, M. (2016). Soil bacteria population dynamics following stimulation for ureolytic microbial-induced $CaCO_3$ precipitation. *Environmental Science & Technology*, *50*(2), 616–624. https://doi.org/10.1021/acs.est.5b04033

Gomez, M. G., Graddy, C. M., DeJong, J. T., & Nelson, D. C. (2019). Biogeochemical changes during bio-cementation mediated by stimulated and augmented ureolytic microorganisms. *Scientific Reports*, *9*(1), 11517. https://doi.org/10.1038/s41598-019-47973-0

Houba, V. J. G., Temminghoff, E. J. M., Gaikhorst, G. A., & Van Vark, W. (2000). Soil analysis procedures using 0.01 M calcium chloride as extraction reagent. *Communications in Soil Science and Plant Analysis*, *31*(9–10), 1299–1396. https://doi.org/10.1080/00103620009370514

IEA. (2020). *Global energy review 2020*. IEA. https://www.iea.org/reports/global-energy-review-2020 Licence: CC BY 4.0.

IPBES. (2019). Global assessment report on biodiversity and ecosystem services of the intergovernmental science-policy platform on biodiversity and ecosystem services. In E. S. Brondizio, J. Settele, S. Díaz, & H. T. Ngo (Eds.), *IPBES secretariat* (p. 1148). https://doi.org/10.5281/zenodo.3831673

IPCC. (2019). Technical Summary, 2019. In P. R. Shukla, J. Skea, E. Calvo Buendia, V. Masson-Delmotte, H.-O. Pörtner, D. C. Roberts, P. Zhai, R. Slade, S. Connors, R. van Diemen, M. Ferrat, E. Haughey, S. Luz, S. Neogi, M. Pathak, J. Petzold, J. Portugal Pereira, P. Vyas, E. Huntley, K. Kissick, M. Belkacemi & J. Malley (Eds.), *Climate change and land: An IPCC special report on climate change, desertification, land degradation, sustainable land management, food security, and greenhouse gas fluxes in terrestrial ecosystems* In Press. https://www.ipcc.ch/srccl/cite-report/

IPCC. (2021). In V. Masson-Delmotte, P. Zhai, A. Pirani, S. L. Connors, C. Péan, S. Berger, N. Caud, Y. Chen, L. Goldfarb, M. I. Gomis, M. Huang, K. Leitzell, E. Lonnoy, J. B. R. Matthews, T. K. Maycock, T. Waterfield, O. Yelekçi, R. Yu, & B. Zhou (Eds.), *Climate change 2021: The physical science basis. Contribution of working group I to the sixth assessment report of the intergovernmental panel on climate change* (p. 2391). Cambridge University Press. https://doi.org/10.1017/9781009157896

ISO 11277. (1998). *Soil quality—Determination of particle size distribution in mineral soil material—Method by sieving and sedimentation*. International Organization for Standarization. https://doi.org/10.31030/9283499

Kim, D. J., Lee, D. I., & Keller, J. (2006). Effect of temperature and free ammonia on nitrification and nitrite accumulation in landfill leachate and analysis of its nitrifying bacterial community by FISH. *Bioresource Technology*, *97*(3), 459–468. https://doi.org/10.1016/j.biortech.2005.03.032

Lapierre, F. M., Schmid, J., Ederer, B., Ihling, N., Büchs, J., & Huber, R. (2020). Revealing nutritional requirements of MICP-relevant Sporosarcina pasteurii DSM33 for growth improvement in chemically defined and complex media. *Scientific Reports*, *10*(1), 22448. https://doi.org/10.1038/s41598-020-79904-9

Meiklejohn, J. (1952). Minimum phosphate and magnesium requirements of nitrifying bacteria. *Nature*, *170*(4339), 1131. https://doi.org/10.1038/1701131a0

Menegat, S., Ledo, A., & Tirado, R. (2022). Greenhouse gas emissions from global production and use of nitrogen synthetic fertilisers in agriculture. *Scientific Reports*, *12*(1), 1–13. https://doi.org/10.1038/s41598-022-18773-w

Millo, C., Dupraz, S., Ader, M., Guyot, F., Thaler, C., Foy, E., & Ménez, B. (2012). Carbon isotope fractionation during calcium carbonate precipitation induced by ureolytic bacteria. *Geochimica et Cosmochimica Acta*, *98*, 107–124. https://doi.org/10.1016/j.gca.2012.08.029

Montoya, B. M., DeJong, J. T., & Boulanger, R. W. (2014). Dynamic response of liquefiable sand improved by microbial-induced calcite precipitation. In *Bio-and chemo-mechanical processes in geotechnical engineering: Géotechnique symposium in print 2013* (Vol. 63, pp. 125–135). ICE Publishing. https://doi.org/10.1680/geot.SIP13.P.019

Norton, J. M. (2011). Diversity and environmental distribution of ammonia-oxidizing bacteria. In B. B. Ward, D. J. Arp, & M. G. Klotz (Eds.), *Nitrification Ammonia-Oxidizing Bacteria* (pp. 39–55). ASM Press. https://doi.org/10.1128/9781555817145.ch3

Okyay, T. O., Nguyen, H. N., Castro, S. L., & Rodrigues, D. F. (2016). CO_2 sequestration by ureolytic microbial consortia through microbially-induced calcite precipitation. *Science of the Total Environment*, *572*, 671–680. https://doi.org/10.1016/j.scitotenv.2016.06.199

Okyay, T. O., & Rodrigues, D. F. (2015). Biotic and abiotic effects on CO_2 sequestration during microbially-induced calcium carbonate precipitation. *FEMS Microbiology Ecology*, *91*(3), fiv017. https://doi.org/10.1093/femsec/fiv017

Pagani, G., & Zardi, U. (1995). Process for urea production. United States Patent no. US6150555A. https://patents.google.com/patent/US6150555A/en

Ramnarine, R., Voroney, R. P., Wagner-Riddle, C., & Dunfield, K. E. (2011). Carbonate removal by acid fumigation for measuring the $\delta^{13}C$ of soil organic carbon. *Canadian Journal of Soil Science*, *91*, 247–250. https://doi.org/10.4141/cjss10066

Sahrawat, K. L. (2008). Factors affecting nitrification in soils. *Communications in Soil Science and Plant Analysis*, *39*(9–10), 1436–1446. https://doi.org/10.1080/00103620802004235

Stein, L. Y., & Nicol, G. W. (2018). Nitrification. In *eLS*. John Wiley & Sons, Ltd. https://doi.org/10.1002/9780470015902.a0021154.pub2

Stocks-Fischer, S., Galinat, J. K., & Bang, S. S. (1999). Microbiological precipitation of $CaCO_3$. *Soil Biology and Biochemistry*, *31*(11), 1563–1571. https://doi.org/10.1016/S0038-0717(99)00082-6

Tsesarsky, M., Gat, D., & Ronen, Z. (2016). Biological aspects of microbial-induced calcite precipitation. *Environmental Geotechnics*, *5*(2), 69–78. https://doi.org/10.1680/jenge.15.00070

Venterea, R. T., Clough, T. J., Coulter, J. A., Breuillin-Sessoms, F., Wang, P., & Sadowsky, M. J. (2015). Ammonium sorption and ammonia inhibition of nitrite-oxidizing bacteria explain contrasting soil N_2O production. *Scientific Reports*, *5*(1), 12153. https://doi.org/10.1038/srep12153

Warren, L. A., Maurice, P. A., Parmar, N., & Ferris, F. G. (2001). Microbially mediated calcium carbonate precipitation: Implications for interpreting calcite precipitation and for solid-phase capture of inorganic contaminants. *Geomicrobiology Journal*, *18*(1), 93–115. https://doi.org/10.1080/01490450151079833

Whiffin, V. S., Van Paassen, L. A., & Harkes, M. P. (2007). Microbial carbonate precipitation as a soil improvement technique. *Geomicrobiology Journal*, *24*(5), 417–423. https://doi.org/10.1080/01490450701436505

Zamani, A., & Montoya, B. M. (2018). Undrained monotonic shear response of MICP-treated silty sands. *Journal of Geotechnical and Geoenvironmental Engineering*, *144*(6), 04018029. https://doi.org/10.1061/(ASCE)GT.1943-5606.0001861

SUPPORTING INFORMATION

Additional supporting information can be found online in the Supporting Information section at the end of this article.

How to cite this article: Comadran-Casas, C., Brüggemann, N., & Jorat, M. E. (2024). Greenhouse gas fluxes of microbial-induced calcite precipitation at varying urea-to-calcium concentrations. *European Journal of Soil Science*, *75*(3), e13516. https://doi.org/10.1111/ejss.13516